Nanocomposite Materials for Radionuclide Sequestration from Groundwater Environments

Simona E. Hunyadi Murph

Abstract The half-lives of radionuclides range from fractions of a second to billions of years. Since no practical method of altering radioactive decay exists, and since exposure to either the energy emitted from radioactive decay or chemical properties of radionuclides poses dire health risks, radioactive materials must be segregated and controlled. The capture, treatment, and disposition of radioactive materials remain an extraordinary challenge. In here, we focus our attention on the synthesis and characterization of a unique class of nanocomposite materials that have potential for removal of radionuclide contamination. Specifically, we report a simple approach to decorate the surface of iron-based (Fe/Fe_xO_y) material with various nano-catalysts. Specifically, copper (Cu), tin (Sn), and silver (Ag) nanoparticles were prepared through two different reduction approaches, namely, citrate and cetyltrimethylammonium bromide (CTAB) methods, on the iron-based material surface. All samples were characterized by a variety of analytical tools, which included scanning electron microscopy (SEM), electron-dispersive X-ray microanalysis (EDS), and EDS mapping to elucidate materials' morphology as well as nano-catalysts' loading and location on the iron-based structures.

Keywords Nanocomposite · Radionuclides · Bimetallic compounds · Sequestration

Introduction

The radioactive nuclides have half-lives ranging from fractions of a second to minutes, hours or days, through to billions of years [1]. Since no practical method of altering radioactive decay exists, and since exposure to either the energy emitted from radioactive decay or chemical properties of radionuclides poses dire health

S. E. Hunyadi Murph (✉)
Savannah River National Laboratory, Aiken, SC 29808, USA
e-mail: Simona.Murph@srnl.doe.gov

University of Georgia, Athens, GA 30602, USA

B. Wisner et al. (eds.), *Composite Materials*, The Minerals, Metals & Materials Series,
https://doi.org/10.1007/978-3-031-50180-7_5

risks, radioactive materials must be segregated and controlled. The nature, volume, and magnitude of radioactive materials are vast and diverse. For example, at the Savannah River Site (SRS), during nuclear material production operations, over 37 million gallons of high-level nuclear waste (HLW), including mixtures of radioactive technetium, cesium, iodine, uranium, plutonium, strontium, etc., were generated as a byproduct of nuclear weapons production [2]. As expected, the stewardship, disposition, and environmental cleanup of nuclear materials are not trivial. It requires sophisticated and operationally complex materials and technologies to effectively isolate them from the environment. Improper treatment and handling would result in significant consequences to the environment [3].

Understanding the intricacies of the radionuclides fate, transport, and performance in the ecosystem is critical for the development of efficient strategies to protect the environment and human health. Therefore, the greatest problems associated with nuclear waste are related to the efficient capture, long-term storage, and disposal of the waste in a non-toxic form [4].

Almost all nuclear operations use sorption technologies to reduce waste volume or to recover key valuable elements or isotopes [5, 6]. Physical or chemical approaches are largely employed for removal of the radioactive elements from waste solutions through the use of adsorbents, absorbents, and ion exchange materials [7]. Technetium-99, a fission product of uranium-238 and a beta emitter, is a major contaminant at nuclear power plants that has been unintentionally released in the environment [8]. Zero valent iron was efficiently used as an effective remediation agent for radioactive Tc decontamination [6, 9]. A micelle directing surfactant, such as cetyltrimethylammonium bromide, was also used for capturing Tc moieties (TcO_4^-) [10]. Moreover, monosodium titanate material is currently used as a baseline sorbent for the removal of other radioactive contaminants, such as Sr-90 and alpha-emitting radionuclides at SRS [7].

Significant challenges remain, however, in the development of deployable techniques with high sensitivity and selectivity for the efficient treatment of radionuclides. This is due to the complex and challenging environments in which these technologies must operate, i.e. high/low pH, temperature/pressure fluctuations, radionuclide mixtures, solvents, neutralizing media, etc. Therefore, in order to accelerate the cleanup efforts, novel materials and technologies are still needed. Among the many classes of candidate materials, nanocomposite materials possess unique properties that could address several limitations and lifecycle schedules related to the nuclear waste materials processing [11, 12]. Nanomaterials' distinctive properties arise from their improved physical and chemical properties imparted over their single-component counterparts [13, 14]. Coupling materials with disparate functionalities and distinct properties into a single, hybrid/multifunctional operating material open the door to a myriad of possibilities and applications for enhanced detection, imaging, manipulation, encapsulation, etc. [15]. Additionally, the high surface area, ease of surface engineering, and diverse likelihoods for interfacial modifications make them highly sought for cleanup purposes [16]. As an example, we developed novel nanocomposite materials in the form of gold-monosodium titanate that not only

capture the radioactive nuclides, but also determine the concentration of the radioactive sorbate in both solution and while captured onto the monosodium titanate solids. This innovative nanotechnology is deployable, cost-effective, and doesn't generate additional waste. It diminishes potential radiation exposure and reduces processing time for the sample preparation and analysis [7, 17].

In here, we focus our attention on the synthesis and characterization of a unique class of nanocomposite materials that could be used for the removal of radionuclide contaminants. Specifically, copper (Cu), tin (Sn), and silver (Ag) nanoparticles were prepared through two different reduction approaches, namely, citrate and cetyltrimethylammonium bromide (CTAB) methods, on the iron-based (Fe/FexOy) material. All samples were characterized by a variety of analytical tools, which included scanning electron microscopy (SEM), electron-dispersive X-ray microanalysis (EDS), and EDS mapping to elucidate materials' morphology as well as nano-catalysts' loading and location on the iron-based structures.

Experimental Details

Materials: All chemicals were purchased from Sigma-Aldrich. Porous iron material was provided by Höganäs Environmental Solutions (Cary, NC, USA). All glasswares used in the following protocols were cleaned with aqua regia and then rinsed with deionized water. A neodymium magnet was used to separate magnetic materials from aqueous solutions.

Fabrication and Characterization: The iron-based material was used as a template for creation of composite material by a straightforward wet chemical method that is amenable for scaling up. All nanoparticles were produced by reduction approaches as previously reported by us while using iron-based material as supports. Basically, metal ions were reduced by either sodium citrate or sodium borohydride in the presence of surfactants or reducing/capping reagents, such as cetyltrimethylammonium bromide (CTAB) or sodium citrate. In the case of the citrate reduction synthesis approach, 1.25×10^{-4} M metal ions was heated to boiling and 1 wt % reducing agent (citrate) solution was added in the presence of 0.1 g of iron-based material. In the case of the CTAB approach, 0.1 g of iron-based material was incubated in an aqueous solution of CTA with a 0.1 M concentration. Next, metal salt 250ul of 0.01 M were introduced into the flask while stirring at room temperature for 15 min. Under vigorous stirring, 600ul of sodium borohydride 0.01 M was added to this solution. Stirring continued for an additional 15 min. Samples were washed after 24 h and dried. Dried samples were placed on copper double tape and imaged with a Hitachi SU8200 Scanning Electron Microscope (SEM) coupled with Energy-Dispersive X-Ray Spectroscopy (EDS) to evaluate nanomaterial morphologies and compositions.

Results and Discussion

Characterization of Iron-Based Materials

Iron-based materials were used here as a template for creation of bimetallic catalytic materials with tailored and tunable structural, optical, and surface properties. Typically, zero valent iron material oxidizes upon oxygen and/or water exposure. Therefore, while not investigated in this study, it is postulated that the template material is a mixture of zero valent iron and iron oxide (Fe/Fe_xO_y) material. It was reported that the presence of hydroxyl radical, superoxide radical, and ferryl ion species enhances material's reactivity [18]. Consequently, this is beneficial for water treatment.

The template, i.e. Fe/FexOy material, was sonicated in either water or sodium citrate before decoration with metallic nanoparticles. Upon 10–15-min sonication, no significant changes were recorded to the material's pore structures and morphology. The material displays unique morphologies with irregular tubular structures and various pore-like and "hollow" environments. The tubular structures have variable configurations and geometries with the diameter ranging from around 1–4 um in size. The pore structure is of particular interest as it is beneficial during treatment of liquid nuclear waste (Fig. 1). Nitrogen sorption isotherm indicated that Fe/FexOy material has a BET surface area of 0.95 m^2/g, pore volume of 0.0068 mL/g, and an average pore diameter of 364 Å [4]. Energy-dispersive X-ray analysis (EDS) shows that over 90% of the material contains elemental Fe with other small percentage of impurities or support elements, i.e. Al, C.

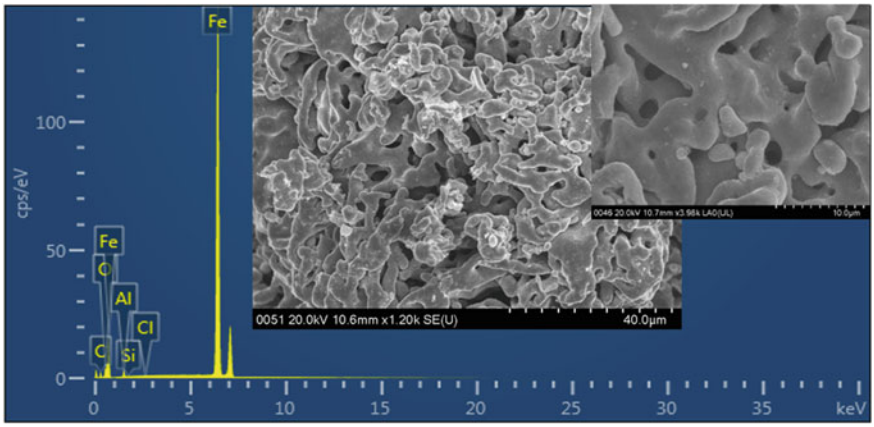

Fig. 1 SEM and EDS data collected on porous iron support materials

Production and Characterization of Nanoscale Decorated Fe/FexOy Materials

Addition of a second metal onto the Fe/FexOy material, especially at the nanoscale, offers significant benefits for water remediation developments. For example, the presence of a nanoscale metal boosts material's reactivity though increased reductive properties and/or catalytic capabilities [19, 20]. These enhanced characteristics were successfully exploited for cleanup efforts, namely, sequestration and decomposition of organic and heavy metal contaminates [21–23]. The presence of a second metal, especially at the nanoscale, facilitates the efficient flow of electron transfer between iron and contaminants. Bimetallic materials also open the door to selectivity through tailored surface functionalization. For example, one could promote targeted sequestration pathways by using various bifunctional linkers for specific interactions, i.e. positive/negative surface charge, hydrophilic/hydrophobic surfaces, etc. Nanomaterials are of particular interests as sequestering agents due to their favorable properties comparing with the bulk materials [24, 25]. Nanoscale materials have an increased surface area when compared to counter bulk materials [26]. A significant portion of atoms are exposed to the environment and available for reactions. Therefore, enhanced reaction kinetics can be obtained by simply using nanoscale materials. Moreover, the surface atoms in nanomaterials have higher energy (due to under-coordination) than the bulk atoms making them highly reactive. Therefore, nanomaterials have higher remediation capacities than the bulk nanomaterials. Nanomaterials also serve as efficient catalysts/photocatalysts or storage media to boost chemical reactions [27]. Either through manipulation of size, shape, and/or composition, nanoscale material's properties can be tailored to drive specific and/or enhanced photo-catalytic or thermo-catalytic reactions [28, 29]. For example, titania nanoparticles are active only in the UV region of the spectrum [30]. By coupling titania to a second component, gold nanoparticles, the photo-catalytic response is enhanced from the UV to the Vis region of the spectrum, leading to enhanced reactivity [31]. Moreover, by decorating iron oxide with Au nanoparticles, we discovered that the nanocomposite material $Fe_2O_3 - Au$ efficiently transduces heat from light through plasmonic absorbance more efficiently than Au alone. This phenomenon was exploited to demonstrate the photothermal catalytic reduction of 4-nitrophenol [26]. Iron-based nanomaterials were successfully employed for removal of organic compounds, heavy metals, and radioactive contaminants [32].

Three different metallic nanoparticles, namely, Cu, Sn, and Ag were produced onto Fe/FexOy materials by straightforward wet chemical reduction methods. Basically, metal salts were reduced in water, in air with a reducing agent to yield spherical nanoparticles onto the porous iron substrates [11]. Nanoparticle production follows the typical four steps: [12] (a) nucleation step, (b) growth, (c) ripening, and (d) rapid consumption of residual precursors [33]. The experimental parameters used during the synthesis procedure, such as reduction rates of the metal precursors, temperature, reductant-to-precursor ratio, ligands, and strength of reductant, all have an effect on the final product. More exactly, the specific geometry, size, and crystallinity can be

manipulated by the selection of these components. Therefore, minute changes to the amount, order, or timing significantly impact the nanoparticle's optical and physical properties.

Decoration of Cu, Sn, and Ag nanoparticles onto Fe/FexOy was monitored by scanning electron microscopy (SEM) (Fig. 2). Despite the diverse non-uniform surface condition, SEM images show that all nanoparticles are distributed over the entire Fe surface, including inside the pores of these structures. Noticeable differences in nanoparticles size and morphologies were recorded. In the case of Cu and Sn, the CTAB procedure produces well-defined nanostructures monodispersed in size with diameters of approximatively 100 nm on the surface of iron structures. In comparison, the citrate approach generates irregular nanostructures with a fair set of aggregates and well-dispersed structures on the support.

In the case of the silver nanostructures, however, the citrate approach generated better defined nanostructures with diameters in the range of 250 and 150 nm for Cu and Sn, respectively. A very limited number of aggregates were produced during the citrate approach. The presence of the metal nanoparticle on the iron structures often leads to a more efficient flow of electrons from the sorbent to the environment leading to faster processes. Additionally, addition of a secondary metal on the support increases the lifetime and reusability of the sorbent. Additionally, a limited amount of nanomaterial is needed to enhance the sorbent's efficiency. These benefits coupled with one's ability to produce nanomaterials via solution chemistries reduce material's cost and limit the amount of waste produced.

Particle-size distribution determined by measuring individual particles and clustered nanoparticles using scanning electron micrographs is displayed in Table 1. Moreover, the elemental composition of the nanocomposite structures was evaluated by the energy-dispersive X-ray analysis (EDS). These results confirm the presence of elements of interest, Cu, Sn, Ag, and Fe, as described in Table 1.While EDS is a semi-quantitative analysis, the data shows that the amount of nanoparticle loading varies based on the procedure used and elemental composition. In the case of Cu and Sn, the loading capacity doubled when the CTAB synthesis approach was used. That could be related to CTAB's ability to form micelle and/or promote electrostatic interactions with the iron support. It is certainly possible that the porous iron surface is oxidized with reticent iron oxide/hydroxide ions on the surface due to deprotonated Fe-OH surfaces. This is in agreement with our previous studies in which iron oxide nanoparticles produced by burning iron metal had a negative surface charge of -11 mV. In the case of silver nanoparticles, however, the loading capacity is five times larger when the citrate approach is used when compared with CTAB approach. It is believed that the nanoparticle growth mechanism is different in each case as it could relate to the CTAB tail contribution to the free energy of formation of a bilayer on different metallic nanoparticles [11]. The magnetic properties of the resulting nanocomposite iron support remained intact upon nanomaterial decoration. This key advantage can be strategically used for recovery via the use of a magnet. This is especially beneficial when there is a need to collect and dispose "payloads" at desired location. A representative EDS and EDS mapping of two different materials

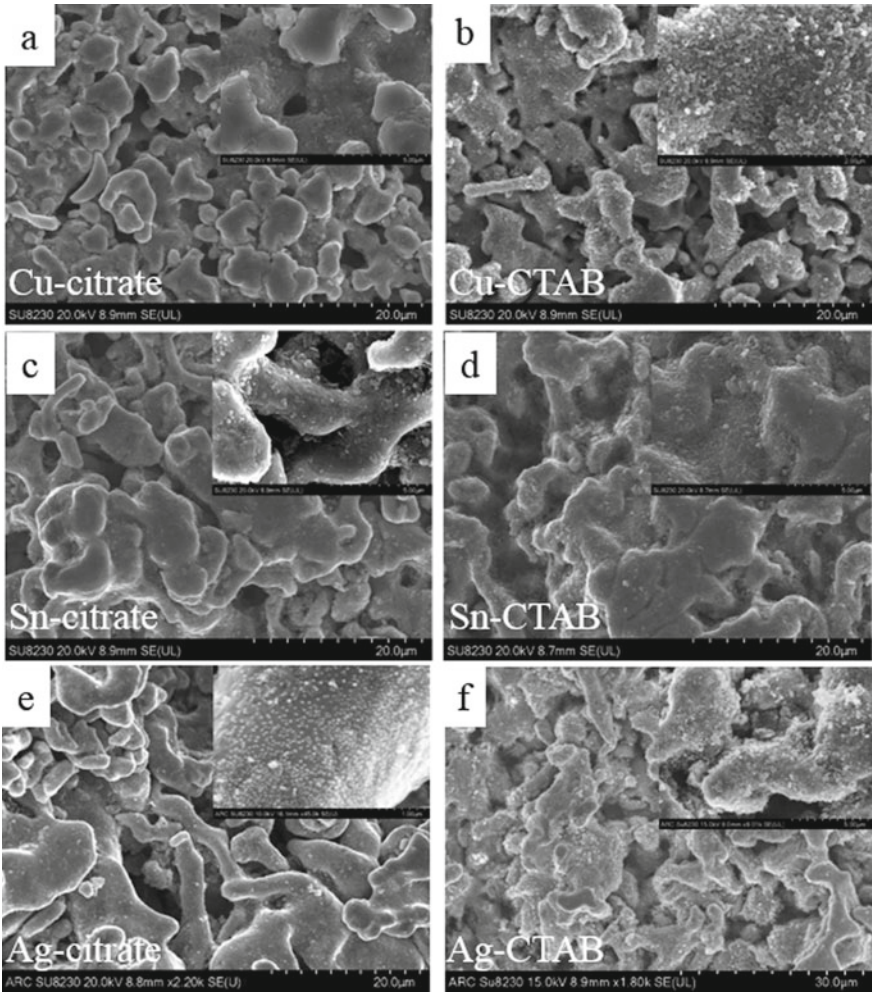

Fig. 2 Electron micrographs of nanomaterials prepared via citrate (left) and CTAB (right) approach: **a**, **b** Cu-Fe/FexOy nanocomposite; **c**, **d** Sn-Fe/FexOy nanocomposite; **e**, **f** Ag-Fe/FexOy nanocomposites

confirmed the presence of the nanomaterials on the entire surface of the iron support (Fig. 3).

Ligand Decoration of Fe/FexOy Structures

The use of different ligands generates materials with different properties. The tunability offered by the ligand's surface charge, i.e. positive, negative, and ligand's

Table 1 Nanoparticles dimensions and compositional analysis

Nanoparticles synthesis procedures	Dimensions (nm)	EDS data ratio (Metal/Fe %)
Cu-citrate	250	0.5
Cu-CTAB	100	1
Sn-citrate	150	0.2
Sn-CTAB	100	0.5
Ag-citrate	30	2
Ag-CTAB	150	0.4

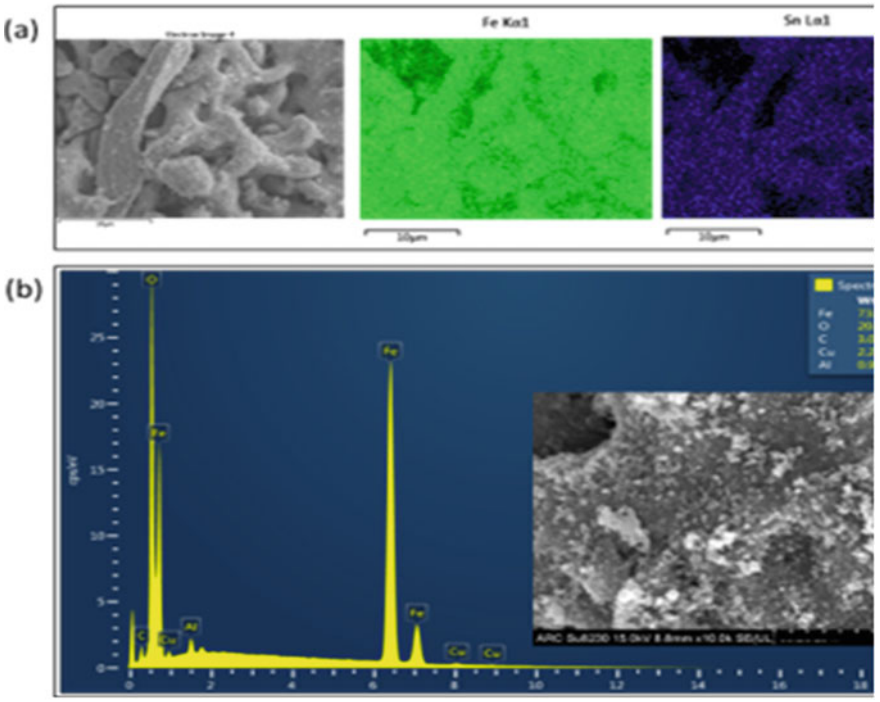

Fig. 3 **a** Representative EDS mapping of Sn-Fe/FexOy nanocomposite showing complete deposition, and **b** EDS and SEM image of Cu-Fe/FexOy nanocomposites

size, or chelation, can be further explored for sequestration of analytes of interest [34]. For example, different surface reactivities, i.e. ligands, but identical composition nanomaterial can be used to target various moieties through tailored electrostatic interactions. The stability and chemistry of the surface ligands can be used to selectively tune analytes' partitioning and permeability.

Two different synthesis approaches were employed in this study to generate bimetallic composite materials: a citrate approach and a CTAB approach. Citrate and

CTAB (Fig. 4) are the most common surfactants used for preparation of nanoparticles. In the case of the citrate approach, sodium citrate serves as both a reducing and a caping agent. In the case of CTAB, a strong reducing agent, sodium borohydride was used. There are major differences between these two approaches. In the citrate synthesis approach, the nanoparticles' surface is negative due to carboxyl groups' capping reagent which renders a negative effective surface charge (–37 mV). This opens the door to metal ion complexation and/or nonspecific electrostatic interactions with the negatively charged particle surface [35]. In contrast, the CTAB synthesis approach generates nanoparticles with a positive surface charge, typically + 30 mV. CTAB has a polar trimethylammonium group at one end making it soluble in aqueous systems and a 16-carbon cetyl tail that has a hydrophobic characteristics. The hydrophobic tail of CTAB interdigitates creating a "zipper-like" bilayer on the nanoparticle's surface. Therefore, the cationic head groups of CTAB are exposed to the environment and convey a positive surface charge of the nanoparticles. The hydrophobic layer can be used to partition water-insoluble moieties from the aqueous environments. CTAB is a micelle directing agent used in the preparation of shape selective metallic nanoparticle, i.e. rods, cubes, and triangles.

By employing these experimental conditions, one could not only preserve the structural integrity of Fe/Fe_xO_y, which is critical in this study but also stimulate specific surface interactions. Surface ligand's molecular structure, length, charge, etc. have a profound effect on material's reactivity, behavior, and stability [36]. Diffusion, interfacial solvent, counterions, and local clustering are just a few examples of parameters that can be used to modulate nanomaterial's surface heterogeneity, electrostatics, and preferential interactions [37]. Solvated ions, interfacial water, and ion distribution have an impact on the biding affinity of nanoparticles to various moieties [38].

Conclusions

We demonstrated production of nanocomposite materials, Cu, Sn, and Ag on Fe/FexOy materials through two different reduction approaches, i.e. citrate or cetyltrimethylammonium bromide (CTAB) approach. These procedures lead to the production of materials with different surface properties which can be further explored for selective sequestration of analytes of interest. Depending on the procedure employed, the nanoparticle's amount on Fe/FexOy varied. For example, metal atom concentration increases as follows: Ag < Sn < Cu when the CTAB approach was used. However, in the citrate approach, the highest metal load was silver with a trend of Sn < Cu < Ag. The preparation procedure is straightforward, cost-effective, and materials can be deployed in the field. The Fe/FexOy material retains its integrity and magnetic properties upon second nanometal manufacture. Therefore, these materials can be easily manipulated and placed as strategic locations through the use of a magnet.

Acknowledgements This work was supported by the Laboratory Directed Research and Development (LDRD) program within the Savannah River National Laboratory (SRNL). This work was produced by Battelle Savannah River Alliance, LLC under contract no. 89303321CEM000080 with the U.S. Department of Energy. Publisher acknowledges the U.S. Government license to provide public access under the DOE Public Access Plan (http://energy.gov/downloads/doe-public-access-plan).

References

1. Hunyadi Murph SE, Murph MA (2023) Nuclear fusion: the promise of endless energy. Phys Sci Rev 8(10):3095–3118. https://doi.org/10.1515/psr-2021-0069
2. Chew D et al (2016) SRR-LWP-2009–00001, rev.20, Savannah River Site
3. Gerdes K et al (2009) SRS salt waste processing facility technology readiness assessment
4. Hunyadi Murph SE et al (2017) Nanoparticle treated stainless steel filters for metal vapor sequestration. JOM 69:162–172. https://doi.org/10.1007/s11837-016-2206-5
5. Larsen G et al, Radiation detectors employing contemporaneous detection and decontamination, US20200395140A1. https://patents.google.com/patent/US20200082954A1/en
6. Hunyadi Murph SE et al, Detection and mitigation of radionuclides in the environment: toward a clean ecosystem.TMS 2023 152nd annual meeting & exhibition supplemental proceedings, pp. 715–724. https://doi.org/10.1007/978-3-031-22524-6_64
7. Fondeour F et al (2020) Methods and materials for determination of distribution coefficients for separation materials, 10:598–599. United States Patent: 10598599 (uspto.gov). https://patents.google.com/patent/US10598599B2/en
8. Li D et al (2019) Porous iron material for TcO4- and ReO4- sequestration from groundwater under ambient oxic conditions. J Hazard Mater 374:177–185. https://doi.org/10.1016/j.jhazmat.2019.04.030
9. Mortazavian S et al (2022) Biochar nanocomposite as an inexpensive and highly efficient carbonaceous adsorbent for hexavalent chromium removal. Materials 15(17):6055. https://doi.org/10.3390/ma15176055
10. Hunyadi Murph SE, Schyck S, Lawrence K (2022) Engineered nano-antenna susceptor as efficient platforms for efficient uptake and release of analytes. In: Srivatsan TS, Rohatgi PK, Hunyadi Murph S (eds) Metal-matrix composites. The minerals, metals & materials series. Springer, Cham. https://doi.org/10.1007/978-3-030-92567-3_22
11. Hunyadi Murph SE, Larsen G, Coopersmith K (2017) Anisotropic and shape-selective nanomaterials: structure-property relationships. Springer Nature, pp 1–470. https://doi.org/10.1007/978-3-319-59662-4
12. Hunyadi Murph SE et al (2013) Patchy silica-coated silver nanowires as SERS substrates. J. Nanopart Res 15(6):1607. https://doi.org/10.1007/s11051-013-1607-4
13. Hunyadi Murph SE, Gaulden P (2022) Novel nanophotocatalysts for detection and remediation of contaminated ecosystems. In: Srivatsan TS, Rohatgi PK, Hunyadi Murph S (eds) Metal-matrix composites. The minerals, metals & materials series. Springer, Cham, pp 335–349. https://doi.org/10.1007/978-3-030-92567-3_21
14. Tao C et al (2007) Surface morphology and step fluctuations on silver nanowires. Surf Sci 601:4939. https://doi.org/10.1016/j.susc.2007.08.023
15. Hunyadi Murph SE et al (2011) Synthesis, functionalization, characterization and application of controlled shape nanoparticles in energy production, fluorine-related nanoscience with energy applications. ACS Symposium Series, vol 1064, Chapter 8, pp 127–163. https://doi.org/10.1021/bk-2011-1064.ch008
16. Hunyadi Murph SE et al (2012) Metallic and hybrid nanostructures: fundamentals and applications, in applications of nanomaterials. In: Govil JN (ed) Nanomaterials and nanostructures. series Studium Press LLC, USA

17. Hunyadi Murph SE, Majidi V (2021) Systems and methods for manufacturing nano-scale materials US Patent US20210380405A1. https://patents.google.com/patent/US20210380405A1/en
18. Greenlee LF et al (2012) Kinetics of zero valent iron nanoparticle oxidation in oxygenated water. Environ Sci Technol 46:12913–12920
19. Lien HL, Zhang WX (2007) Nanoscale Pd/Fe bimetallic particles: catalytic effects of palladium on hydrodechlorination. Appl Catal B – Environ 77:110–116
20. Wang CB, Zhang WX (1997) Synthesizing nanoscale iron particles for rapid and complete dechlorination of TCE and PCBs. Environ Sci Technol 31:2154–2156
21. Crane RA, Pullin H, Macfarlane J, Silion M, Popescu IC, Andersen M, Calen V, Scott TB (2015) Field application of iron and iron-nickel nanoparticles for the ex situ remediation of a uranium-bearing mine water effluent. J Environ Eng 141(8)
22. Hu CY, Lo SL, Liou YH, Hsu YW, Shih KM, Lin CJ (2010) Hexavalent chromium removal from near natural water by copper-iron bimetallic particles. Water Res 44(10):3101–3108
23. Zhou T, Li YZ, Lim TT (2010) Catalytic hydrodechlorination of chlorophenols by Pd/Fe nanoparticles: comparisons with other bimetallic systems, kinetics and mechanism. Sep Purif Technol 76(2):206–214
24. Hunyadi Murph SE (2011) One-dimensional plasmonic nano-photocatalysts: synthesis, characterization and photocatalytic activity. In: Tachibana Y (ed) Solar hydrogen and nanotechnology VI. Proceedings of SPIE. vol 8109, 81090T, pp 1–11. https://doi.org/10.1117/12.893029
25. Hunyadi Murph SE, Murphy CJ (2013) Patchy silica-coated silver nanowires as SERS substrates. J Nanoparticle Res 15(6):1607. https://doi.org/10.1007/s11051-013-1607-4
26. Hunyadi Murph SE, Larsen G, Lascola R (2016) Multifunctional hybrid Fe2O3-Au nanoparticles for efficient plasmonic heating. J Visual Exp (JOVE) 108:e53598. https://doi.org/10.3791/53598
27. Hunyadi Murph SE, Lawrence K, Sessions H, Brown M, Larsen G (2020) Controlled release of hydrogen isotopes from hydride-magnetic nanomaterials. ACS Appl Mater Interfaces 12(8):9478–9488. https://doi.org/10.1021/acsami.0c00887
28. Hunyadi Murph SE et al (2021) Efficient thermal processes using alternating electromagnetic field for methodical and selective release of hydrogen isotopes. Energy Fuels 35:3438–3448. https://doi.org/10.1021/acs.energyfuels.0c03704
29. Hunyadi Murph SE et al, Nanocomposite materials for accelerating decarbonization. TMS 2023 152nd annual meeting & exhibition supplemental proceedings, pp. 748–757. https://doi.org/10.1007/978-3-031-22524-6_68
30. Hunyadi Murph SE (2020) Shape-selective mesoscale nanoarchitectures: preparation and photocatalytic performance. Catalysts 10:532. https://doi.org/10.1007/978-3-319-59662-4
31. Srivatsan TS, Harrigan WC, Hunyadi Murph SE (2021) Metal-matrix composites: advances in analysis, measurement, and observations, p 281. https://doi.org/10.1007/978-3-030-65249-4
32. Srivatsan TS, Rohatgi PK, Hunyadi Murph SE (2022) Metal-matrix composites: advances in processing, characterization, performance and analysis. Springer Nature, pp 1–385. https://doi.org/10.1007/978-3-030-92567-3
33. Larsen G et al (2016) Multifunctional Fe2O3-Au nanoparticles with different shapes: enhanced catalysis, photothermal effects, and magnetic recyclability. J Phys Chem C 120:15162–15172. https://doi.org/10.1021/acs.jpcc.6b03733
34. Gankanda A, Rentz NS, Greenlee LF (2019) Greenlee influence of ligand size and chelation strength on zerovalent iron nanoparticle adsorption and oxidation behavior in the presence of water vapor and liquid water. J Phys Chem C 123(4):2474–2487
35. Hunyadi Murph SE (2012) Manganese–doped gold nanoparticles as positive contrast agents for magnetic resonance imaging (MRI). J Nanopart Res 14:658–659. https://doi.org/10.1007/s11051-011-0658-7
36. Cui AY, Cui Q (2021) Modulation of nanoparticle diffusion by surface ligand length and charge: analysis with molecular dynamics simulations. J Phys Chem B 125(17):4555–4565. https://doi.org/10.1021/acs.jpcb.1c01189

37. Liang D et al (2020) Ligand length and surface curvature modulate nanoparticle surface heterogeneity and electrostatics. J Phys Chem C 124:24513–24525. https://doi.org/10.1021/acs.jpcc.0c08387
38. Liang, D at al (2020) Interfacial water and ion distribution determine ζ potential and binding affinity of nanoparticles to biomolecules. Nanoscale 12(35):18106–18123. https://doi.org/10.1039/D0NR03792C
39. Hunyadi Murph SE, Larsen G, Coopersmith K (2017) Anisotropic and shape-selective nanomaterials: structure-property relationships. Springer Nature. https://doi.org/10.1007/978-3-319-59662-4